SLAC-PUB-16943

Understanding trends in electrochemical CO_2 reduction rates

Xinyan Liu[Δ,†], Jianping Xiao[Δ,†], Hongjie Peng[†,§], Xin Hong[†,#] , Karen Chan[†, ‡], Jens K. Nørskov*,[†, ‡]

[†]SUNCAT Center for Interface Science and Catalysis, Department of Chemical Engineering, Stanford University, Stanford, California 94305, United States

[‡]SUNCAT Center for Interface Science and Catalysis, SLAC National Accelerator Laboratory, 2575 Sand Hill Road, Menlo Park, California 94025, United States

[§]Department of Chemical Engineering, Tsinghua University, Beijing 100084, China

[#]Department of Chemistry, Zhejiang University, Hangzhou 310027, China

[Δ]These authors contributed equally

*corresponding author: norskov@stanford.edu

We present an understanding of trends in electrocatalytic activity for CO_2 reduction over different metal catalysts that rationalize a number of experimental observations including the selectivity with respect to the competing hydrogen evolution reaction. We also identify two design criteria for new catalysts. The understanding is based on density functional theory calculations of activation energies for electrochemical CO reduction as a basis for an electrochemical kinetic model of the process. We develop scaling relations relating transition state energies to the CO adsorption energy and determine the optimal value of this descriptor to be very close to that of Cu.

Electrochemical CO_2 reduction to hydrocarbons and alcohols presents one of the great challenges in chemistry. There are known electrode catalysts that can facilitate the process, but they are generally very inefficient – large overpotentials are needed to produce significant reaction rates and the selectivity towards the desired products are often low, with hydrogen evolution being the major competing process[1-4]. If we could find materials that are able to catalyze this reaction efficiently, we would have a pathway to making fuels and base chemicals in a sustainable way, thus allowing for a zero-emission energy conversion cycle[5-8].

Recent experimental reports have focused on the detection of the wide range of carbon-based products on transition metal catalysts[2], effects of alloying[4,9,10], meso- and nano-structuring[3,11-13] and electrolyte engineering[14-16] on activity and selectivity, as well as *in situ* spectroscopic detection of reaction intermediates[17,18]. Theoretical works employing density functional theory and various descriptions of the electrochemical interface have usually focused on the mechanism on copper, which is the only pure transition metal capable of reducing CO_2 to alcohols and hydrocarbons at reasonable faradaic efficiencies[19-25]. Computational screening for new catalysts has also been attempted based on scaling relations between reaction intermediates identified using a thermodynamic analysis of the reaction pathway[26-28].

The fact that no catalyst has been found so far that can efficiently catalyze CO_2 electro-reduction to hydrocarbons or alcohols points to a fundamental problem in our current understanding. In

This material is based upon work supported by the U.S. Department of Energy, Office of Science, under Contract No. DE-AC02-76SF00515.

this letter, we present the first *ab initio* kinetic model of CO reduction on transition and noble metals that describes trends in catalytic activity and the selectivity of CO reduction over hydrogen evolution. We are primarily interested in CO_2 reduction to more reduced products than CO, and we therefore focus on CO as the reactant. CO_2 reduction to CO requires considerably lower overpotentials[29], and thermodynamic descriptors have been able to accurately predict active catalysts[30,31].We use density functional theory (DFT) calculations and an explicit solvent model of the electrochemical interface to determine potential-dependent activation energies for electrochemical CO reduction. We show that the transition state energy for the H-CO complex scales linearly with the CO adsorption energy for metal surface catalysts, and identify the H-CO vs. CO scaling as a crucial determinant of catalytic activity. Model turnover frequencies, polarization curves, and selectivity show reasonable agreement with existing experimental data, and suggest stepped sites to dominate the overall activity. On the basis of the kinetic model, we present two design strategies for more active CO_2R catalysts.

We note that direct CO hydrogenation is only one possible pathway. Under the influence of electric fields induced by ions at the interface, CO molecules may also couple directly with each other before hydrogenation leading to C_2 products [19,32,33]. This pathway, which is only likely to contribute to the total rate at fairly low overpotentials, is not included here, and our calculated rates can be viewed as a lower bound on the actual rate at these potentials.

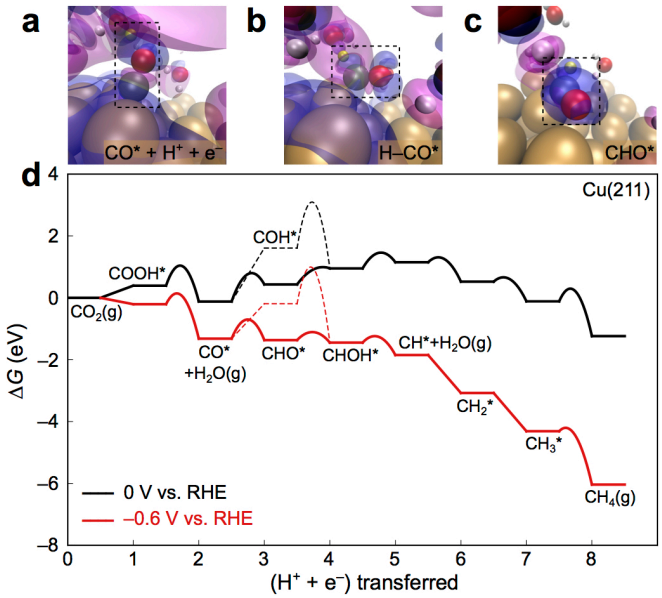

Figure 1 Free energy diagram for the reduction of CO_2 to CH_4 on Cu(211) at 0 V and the thermodynamic limiting potential, –0.6 V vs. RHE. a-c: charge density difference isosurfaces for the rate determining, proton-electron transfer to *CO to form *CHO. *CO, the *H-CO complex, and *CHO have been highlighted with dashed lines. Blue and magenta isosurfaces correspond to charge densities of of –0.001 $eBohr^{-3}$ *and* +0.001 $eBohr^{-3}$, respectively. The isosurfaces illustrate the transfer of positive charge to the negatively charged slab along the reaction pathway.

Figure 1d shows our calculated free energy diagram including activation free energies for a complete series of elementary steps leading from CO_2 to CH_4 (as an example of a possible product) for a stepped Cu(211) surface. We have also included the alternative pathway, CO hydrogenation to COH, which is found to be higher in energy, in contrast to results from

simulations using more approximate estimates of electrochemical barriers[20,21]. The calculation has five components, which are discussed in more detail in the supplementary information (SI):

1) We consider coupled electron-proton reaction steps, assuming that the electron transfer happens on a time-scale much faster than the proton transfer. This is a good approximation since the transition state complexes are tightly coupled to the surface, as illustrated by the projected density of states at the transition state, see SI, Figure S6.
2) Reaction energies of all elementary steps are calculated using the computational hydrogen electrode including an explicit solvent layer. All interaction energies are calculated using error estimation ensembles within the BEEF-vdW functional[34].
3) Activation energies are calculated using an explicit description of the solvent (see Figure 1a-b for the associated charge density difference isosurfaces). All systems consist of a single layer of hydrogen-bonded water and a 3-4 layer transition metal slab. Excess hydrogens in the water layer charge separate into solvated protons in the Helmholtz plane with countercharge in the slab. Barriers were determined using the climbing-image nudged elastic band method[35].
4) Free energies $G=E+E_{ZPE}-TS$ are estimated by including zero point energies and entropy contributions calculated in the harmonic approximation[36]. Transition state energies are corrected by the zero point energies of transition state complexes, but no configurational entropies are included in accordance with transition state theory. All corrections are included in the supplementary info in Tables S1.
5) The potential dependence of the activation energies are calculated as described in Refs. [37,38]. Assuming a SHE work function of 4.4 eV, activation energies are extrapolated to a work function of 4.0 eV, which corresponds to 0 V vs. RHE at pH 7. All activation energies are referenced to the aqueous protons in bulk solution using the computational hydrogen electrode[39].

Figure 1d shows that on Cu(211) the elementary reaction step involving *CO hydrogenation to *CHO has the highest free energy barrier; the corresponding charge density isosurfaces along the reaction pathway are shown in Figure 1a-c. We therefore focus on trends in the rate of CO hydrogenation on other metals and surface structures, in order to understand trends in CO_2 reduction activity. Catalysts far from Cu in the periodic table may have larger activation energies for other elementary steps, in which case CO hydrogenation rate will not be the limiting step and will be an upper bound to the rate. We will show, in agreement with experiment, that the optimum catalyst is close to Cu, which suggests that we describe the region around the optimum well by concentrating on the CO reduction step.

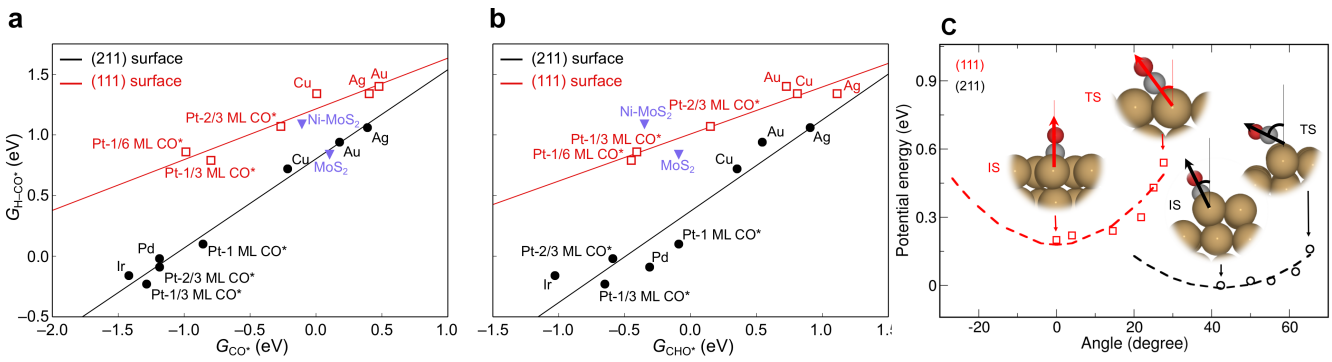

Figure 2 Scaling relations of CO reduction transition state energies on (111) and (211) transition metal facets: a) $G_{\text{H-CO*}}$ vs. $G_{\text{CO*}}$ b) $G_{\text{H-CO*}}$ vs. $G_{\text{CHO*}}$. c) Potential Energy curves for CO adsorbed Cu(111) and Cu(211) as a function of the angle of rotation. For Cu(111) a rotation of adsorbed CO is more energetically costly from initial state to transition state with respect to the stepped Cu(211) surface, which rationalizes the lower transition state energies for stepped surface. All energies are referenced to solvated protons far from the surface at pH=7, electrons at 0 V vs. RHE and gas phase CO at T=300 K, P=1 bar.

In Figure 2, we show the CO reduction transition state free energies at 0 V *vs.* RHE for several metals and coverages, and for two different surface orientations with fcc(111) surfaces representing close-packed facets, and fcc(211) surfaces representing low-coordinated, step-like sites. The transition state energies are plotted as a function of the CO adsorption energy, and there is a clear scaling relation between the two. This is the first identification of a transition state scaling relation for electrochemical CO reduction. The scaling relations are surface structure-dependent, like in thermal surface processes[40].

We then develop a mean field kinetic model to describe the potential-dependent rate of CO reduction to more reduced products. The model includes adsorbate-adsorbate interactions in a self-consistent way[41] (details in the SI). The model is devised to describe trends in catalytic activity. Even if absolute rates are not always quantitatively described by DFT calculations, variations in activity amongst a group of catalysts, such as transition metals, are described considerably better[42]. The reason is that the intrinsic error in DFT calculations tends to be systematic in the sense that if one metal over-binds intermediates or transition states, so do the other metals. Having said that, the model describes the variation of current density and selectivity with potential for Cu quite well. Figure 3 shows the theoretical polarization curves for CO reduction for Cu(100), (111) and (211), as well as the experimental CO_2 reduction curve from Ref. [43] for all products further reduced from CO. A CO backpressure of 1 mbar was estimated[44] based on the molar efficiencies determined in Ref. [43,45], which was used as input for the theoretical model. We include results where the number of step-like sites are in the range observed on single crystal surfaces, 1-5%[46], showing that within the uncertainly of our model (DFT, mean field kinetics, and the number of active sites) and of the experiments (active site area, diffusion limitations) our description is quite good, both in terms of the Tafel slope and the absolute rates.

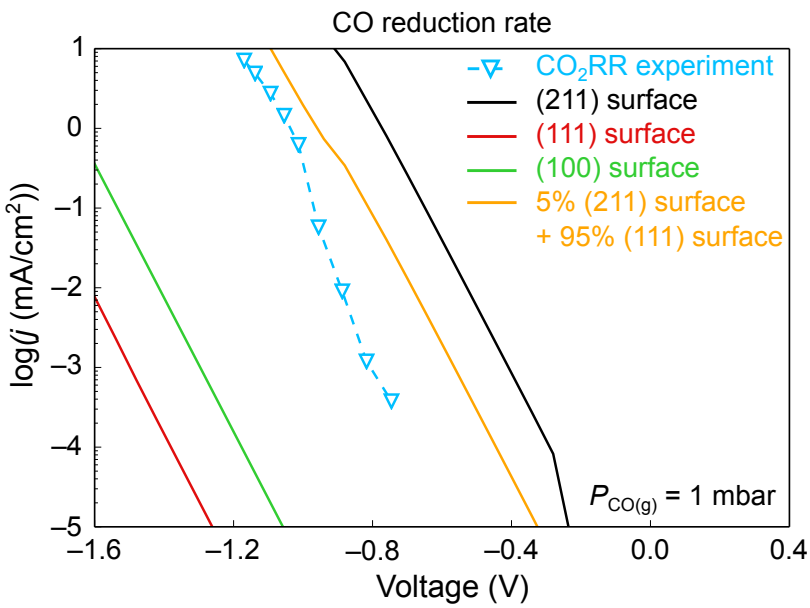

Figure 3 Polarization curves for Cu(100), (111) and (211) facets at pH=7, 1 mbar CO(g) for CO reduction to CH4. Experimental data is from Ref. [2,41,43] for CO_2 reduction for all post-CO products, pH=7, where a backpressure of CO of 1 mbar was estimated[7].

Since the CO adsorption energy defines the activation energies through the scaling relation (Figure 2a), we can derive the rate of electrochemical CO reduction as a function of the CO adsorption energy for two different surface structures, as shown in **Error! Reference source not found.** for potentials –0.5 and –1.0 V *vs.* RHE. All CO adsorption energies for the various metals indicated correspond to that calculated at low-coverage, with 1 *CO per 3x3 sized unit cell. The fact that the low coverage CO adsorption energies are used in the volcano plots is merely a convention to determine which energy we use to characterize a given metal. The error bars on the relative rates, derived from BEEF-vdW ensembles[34], are shown in the SI in Figure S4.

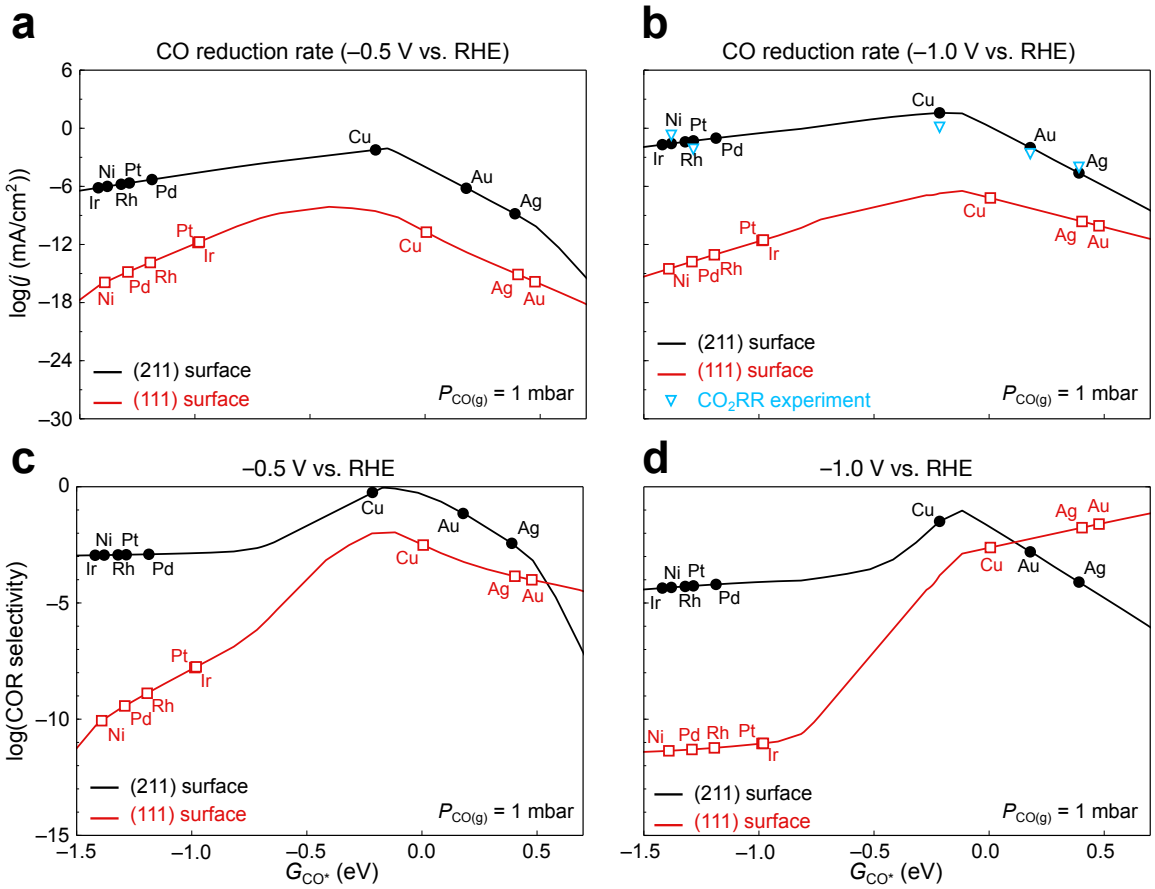

Figure 4 Activity volcanoes for flat (111) and stepped (211) transition metal surfaces as a function of CO binding energy, at a) –0.5 V vs RHE, b) –1.0 V vs RHE, as determined through microkinetic modeling. CO_2 reduction experimental data from Ref. [2,43,45]; CO pressure estimated[47] to be 1 mbar under CO_2 reduction conditions, pH=7. Selectivity towards CO reduction at c) –0.5 V vs RHE, d) –1.0V vs RHE, defined as the rate of CO reduction relative to the sum of the rate of CO reduction and hydrogen evolution.

Error! Reference source not found. Figure 4 shows that according to the model, the stepped (211) surfaces always have a considerably higher activity than the close-packed (111) surfaces for a given CO adsorption energy. The larger catalytic activity of the step-like sites can be traced back to generally lower activation energies (Figure 2a), and can be rationalized by the accessibility of the C end of *CO to the incoming proton (Figure 2c), and the ease with which the *CO rotates towards the transition state. Figure 2c shows the potential energy curves for CO adsorbed on Cu(111) and (211) as a function of the angle of rotation from the initial to transition state. On the (211) surface, the overall angle of rotation between the IS and TS is smaller, and the overall energy change from this rotation is also considerably smaller.

The finding that step-like structures are much more reactive than more close-packed surfaces appears not to be in agreement with experiments on CO reduction on single crystal data[1,48,49]. The question is what the state of the surface is under reaction conditions. Recent electrochemical STM imaging show transition metal surfaces to be highly dynamic under electrochemical conditions[50,51], which complicates the direct comparison with experimental single crystal data. We note that recent experiments on polycrystalline copper show oxidation-reduction cycles to give rise to stepped surfaces active for the low-overpotential production of ethanol.[50]

In Figure 4 (and S4), we include experimental CO_2 reduction data from Ref. [2]. Our model rationalizes a number of experimentally observed trends in CO reduction rates: Cu is the best elemental metal catalyst, and for the weaker binding metals, the lack of CO coverage limits the rate. On the stronger binding side of the maximum, the variation in rate is smaller, in particular for the step sites. The reason is that the slope of the transition state scaling line (slope 0.73) is close to one, meaning that the activation energy $E_a = E_{H\text{-}CO*} - E_{CO*}$ varies only weakly (slope –0.27) with the CO adsorption energy (and hence the metal).

Apart from the rate of $CO_{(2)}$ reduction, the selectivity over the hydrogen evolution reaction (HER) is crucial to the efficiency of $CO_{(2)}$ reduction catalysts. Figure 4c-d shows the selectivity towards COR vs. the total current at –0.5 and –1.0V vs. RHE. On stepped sites, which should dominate the overall activity, our model suggests that only around Cu in terms of CO adsorption energy is there any substantial selectivity towards CO reduction products, consistent with experimental observations[2].

Figure 4 suggests that Cu is close to the optimum both in terms of rate and selectivity. This hypothesis has not been contradicted by experiments so far. The results suggest two strategies for catalyst design. The first option is to increase the number of step-like sites. We suggest that the high activity forms of nano-structured transition metals that have been reported[3,52,53] may in fact result from a larger fraction of steps and edges in these high surface area samples. The importance of special strong-binding sites has been suggested by temperature-programmed desorption of oxide-derived copper.[54] Stabilizing a large fraction of edge and step sites is an important design criterion. As noted above, the dynamic nature of metal surfaces under electrochemical conditions makes it hard to know which sites are on a given surface and even harder to control them.

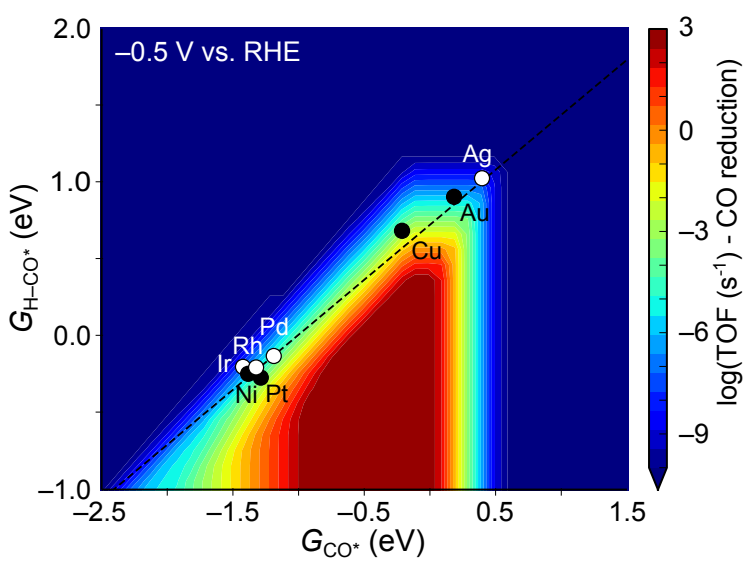

Figure 5 Two dimensional map of the rate of CO reduction as a function of the H-CO transition state energy and the CO binding energy at a potential of –0.5 V vs. RHE.

The other option is to find exceptions to the scaling relation between the H-CO complex and CO in Figure 2a. As indicated in **Error! Reference source not found.**, the rate could be substantially larger if we could find catalysts where the transition state is stabilized for a given CO adsorption energy.

Previously, a purely thermochemical analysis had suggested that the free energy of adsorbed CHO could be used as a simple measure of the activity[55]. On pure transition metal surfaces the H-CO complex does scale with *CHO binding energy (Figure 2b). However, while (doped) MoS_2 stabilizes the CHO binding energies relative to the transition metal scaling relation[28], their corresponding transition states are not stabilized, as shown in Figure 2b. CHO binds to a different site than CO on the sulfides, which decouples the scaling between the two energies. Unfortunately, as shown in Figure S7, the transition state is initial-state like, and therefore this effect cannot be exploited for the transition state energy. We therefore suggest that the CHO adsorption energy can only be used as a descriptor for situations where there is no site change during the process, and that any screening study should begin with the evaluation of the energy of the H-CO transition state complex. This then poses a considerably more stringent design criterion for active catalysts than can be derived from a simple thermodynamic analysis.

In conclusion, we have presented the first kinetic model for electrochemical CO reduction, based on *ab initio*, explicit solvent calculations of the energetics of the elementary steps. This kinetic model gave the first theoretical polarization curves, kinetic activity volcano, and selectivities on a range of transition and noble metals. We showed that the CO reduction activity is dominated by step sites, and that the activity is limited by the scaling relation between the *transition state* for CO hydrogenation and CO binding energies. The latter insight points to a considerably more stringent design criterion for more active catalysts for $CO_{(2)}$ electroreduction than a simple thermochemical analysis. Future work will focus on refinements of the model to investigate effects of C-C coupling, CO dissociation in the case of strongly binding metals, pH and mass transport, and solvation and electrolyte structures.

Acknowledgements

This material is based upon work performed by the Joint Center for Artificial Photosynthesis, a DOE Energy Innovation Hub, supported through the Office of Science of the U.S. Department of Energy under Award Number DE-SC0004993. This research used resources of the National Energy Research Scientific Computing Center, a DOE Office of Science User Facility supported by the Office of Science of the U.S. Department of Energy under Contract No. DE-AC02-05CH11231. H.J.P. acknowledges the China Scholarship Council (CSC) for financial support.

Competing financial interests

Authors declare no competing financial interest.

Author Contributions

X.Y.L., J.P.X., H.J.P, and X.H. contributed calculations, analysis of data, and writing. K.C. and

J.K.N. contributed writing and discussion.

References

1 Hori, Y. in *Modern Aspects of Electrochemistry Modern Aspects of Electrochemistry* (eds Constantinos G. Vayenas, Ralph E. White, & Maria E. Gamboa-Aldeco) 89-189 (Springer New York, 2008).

2 Kuhl, K. P. *et al.* Electrocatalytic Conversion of Carbon Dioxide to Methane and Methanol on Transition Metal Surfaces. *Journal of the American Chemical Society*, doi:10.1021/ja505791r (2014).

3 Li, C. W., Ciston, J. & Kanan, M. W. Electroreduction of carbon monoxide to liquid fuel on oxide-derived nanocrystalline copper. *Nature* **508**, 504-507, doi:10.1038/nature13249 (2014).

4 Torelli, D. A. *et al.* Nickel-Gallium-Catalyzed Electrochemical Reduction of CO2 to Highly Reduced Products at Low Overpotentials. *ACS Catalysis*, doi:10.1021/acscatal.5b02888 (2016).

5 Whipple, D. T. & Kenis, P. J. A. Prospects of CO2 Utilization via Direct Heterogeneous Electrochemical Reduction. *The Journal of Physical Chemistry Letters* **1**, 3451-3458, doi:10.1021/jz1012627 (2010).

6 Singh, M. R., Clark, E. L. & Bell, A. T. Thermodynamic and achievable efficiencies for solar-driven electrochemical reduction of carbon dioxide to transportation fuels. *Proceedings of the National Academy of Sciences*, 201519212, doi:10.1073/pnas.1519212112 (2015).

7 Chen, Y., Lewis, N. & Xiang, C. Operational Constraints and Strategies for Systems to Effect the Sustainable, Solar-Driven Reduction of Atmospheric CO2. *Energy & Environmental Science*, doi:10.1039/C5EE02908B (2015).

8 Verma, S., Kim, B., Jhong, H.-R. M., Ma, S. & Kenis, P. J. A. A Gross-Margin Model for Defining Technoeconomic Benchmarks in the Electroreduction of CO2. *ChemSusChem*, n/a-n/a, doi:10.1002/cssc.201600394 (2016).

9 Rasul, S. *et al.* A Highly Selective Copper–Indium Bimetallic Electrocatalyst for the Electrochemical Reduction of Aqueous CO2 to CO. *Angewandte Chemie*, n/a-n/a, doi:10.1002/ange.201410233 (2014).

10 Yang, H., Yue, Y.-N., Qin, S., Wang, H. & Lu, J. Selective electrochemical reduction of CO2 to adjustable alcohol products by an organically doped alloy catalyst. *Green Chemistry*, doi:10.1039/C6GC00091F (2016).

11 Tang, W. *et al.* The importance of surface morphology in controlling the selectivity of polycrystalline copper for CO2 electroreduction. *Physical Chemistry Chemical Physics* **14**, 76-81, doi:10.1039/C1CP22700A (2011).

12 Hall, A. S., Yoon, Y., Wuttig, A. & Surendranath, Y. Mesostructure-Induced Selectivity in CO2 Reduction Catalysis. *Journal of the American Chemical Society*, doi:10.1021/jacs.5b08259 (2015).

13 Sen, S., Liu, D. & Palmore, G. T. R. Electrochemical Reduction of CO2 at Copper Nanofoams. *ACS Catalysis* **4**, 3091-3095, doi:10.1021/cs500522g (2014).

14 Rosen, B. A. *et al.* Ionic Liquid–Mediated Selective Conversion of CO2 to CO at Low Overpotentials. *Science* **334**, 643-644, doi:10.1126/science.1209786 (2011).

15 Asadi, M. *et al.* Nanostructured transition metal dichalcogenide electrocatalysts for CO2 reduction in ionic liquid. *Science* **353**, 467-470, doi:10.1126/science.aaf4767 (2016).
16 Morris, A. J., McGibbon, R. T. & Bocarsly, A. B. Electrocatalytic Carbon Dioxide Activation: The Rate-Determining Step of Pyridinium-Catalyzed CO2 Reduction. *ChemSusChem* **4**, 191-196, doi:10.1002/cssc.201000379 (2011).
17 Heyes, J., Dunwell, M. & Xu, B. CO2 Reduction on Cu at Low Overpotentials with Surface-Enhanced in Situ Spectroscopy. *The Journal of Physical Chemistry C* **120**, 17334-17341, doi:10.1021/acs.jpcc.6b03065 (2016).
18 Wuttig, A., Yaguchi, M., Motobayashi, K., Osawa, M. & Surendranath, Y. Inhibited proton transfer enhances Au-catalyzed CO2-to-fuels selectivity. *Proceedings of the National Academy of Sciences* **113**, E4585-E4593, doi:10.1073/pnas.1602984113 (2016).
19 Cheng, T., Xiao, H. & Goddard Iii, W. A. The Free Energy Barriers and Reaction Mechanisms for the Electrochemical Reduction of CO on the Cu(100) Surface Including Multiple Layers of Explicit Solvent at pH 0. *J. Phys. Chem. Lett.* (2015).
20 Nie, X., Luo, W., Janik, M. J. & Asthagiri, A. Reaction mechanisms of CO2 electrochemical reduction on Cu(1 1 1) determined with density functional theory. *Journal of Catalysis* **312**, 108--122 (2014).
21 Xiao, H., Cheng, T., Goddard, W. A. & Sundararaman, R. Mechanistic Explanation of the pH Dependence and Onset Potentials for Hydrocarbon Products from Electrochemical Reduction of CO on Cu (111). *Journal of the American Chemical Society* **138**, 483-486, doi:10.1021/jacs.5b11390 (2016).
22 Calle-Vallejo, F. & Koper, M. T. M. Theoretical Considerations on the Electroreduction of CO to C2 Species on Cu(100) Electrodes. *Angew. Chem. Int. Ed.* **52**, 7282--7285 (2013).
23 Hussain, J., Skúlason, E. & Jónsson, H. Computational Study of Electrochemical CO2 Reduction at Transition Metal Electrodes. *Procedia Computer Science* **51**, 1865-1871, doi:10.1016/j.procs.2015.05.419 (2015).
24 Goodpaster, J. D., Bell, A. T. & Head-Gordon, M. Identification of Possible Pathways for C–C Bond Formation during Electrochemical Reduction of CO2: New Theoretical Insights from an Improved Electrochemical Model. *The Journal of Physical Chemistry Letters* **7**, 1471-1477, doi:10.1021/acs.jpclett.6b00358 (2016).
25 Peterson, A. A., Abild-Pedersen, F., Studt, F., Rossmeisl, J. & Nørskov, J. K. How Copper Catalyzes the Electroreduction of Carbon Dioxide into Hydrocarbon Fuels. *Energy Environ. Sci.* **3**, 1311--1315 (2010).
26 Hansen, H. A., Shi, C., Lausche, A. C., Peterson, A. A. & Nørskov, J. K. Bifunctional alloys for the electroreduction of CO2 and CO. *Physical Chemistry Chemical Physics*, doi:10.1039/C5CP07717F (2016).
27 Hahn, C. *et al.* Synthesis of thin film AuPd alloys and their investigation for electrocatalytic CO ₂ reduction. *J. Mater. Chem. A* **3**, 20185-20194, doi:10.1039/C5TA04863J (2015).
28 Hong, X., Chan, K., Tsai, C. & Nørskov, J. K. How Doped MoS2 Breaks Transition-Metal Scaling Relations for CO2 Electrochemical Reduction. *ACS Catalysis*, 4428-4437, doi:10.1021/acscatal.6b00619 (2016).
29 Jovanov, Z. P. *et al.* Opportunities and challenges in the electrocatalysis of CO2 and CO reduction using bifunctional surfaces: A theoretical and experimental study of Au–Cd alloys. *Journal of Catalysis*, doi:10.1016/j.jcat.2016.04.008.

30 Asadi, M. *et al.* Robust carbon dioxide reduction on molybdenum disulphide edges. *Nature Communications* **5**, doi:10.1038/ncomms5470 (2014).
31 Chan, K., Tsai, C., Hansen, H. A. & Nørskov, J. K. Molybdenum sulfides and selenides as possible electrocatalysts for CO2 reduction. *ChemCatChem* **6**, 1899--1905 (2014).
32 Montoya, J. H., Shi, C., Chan, K. & Norskov, J. K. Theoretical Insights into a CO Dimerization Mechanism in CO2 Electroreduction. *The journal of physical chemistry letters* **6**, 2032--2037 (2015).
33 Kortlever, R., Shen, J., Schouten, K. J. P., Calle-Vallejo, F. & Koper, M. T. M. Catalysts and Reaction Pathways for the Electrochemical Reduction of Carbon Dioxide. *The Journal of Physical Chemistry Letters*, doi:10.1021/acs.jpclett.5b01559 (2015).
34 Wellendorff, J. *et al.* Density functionals for surface science: Exchange-correlation model development with Bayesian error estimation. *Physical Review B* **85**, 235149, doi:10.1103/PhysRevB.85.235149 (2012).
35 Henkelman, G., Uberuaga, B. P. & Jónsson, H. A Climbing Image Nudged Elastic Band Method for Finding Saddle Points and Minimum Energy Paths. *J. Chem. Phys.* **113**, 9901--9904 (2000).
36 Cramer, C. J. *Essentials of Computational Chemistry: Theories and Models*. (Wiley, 2013).
37 Chan, K. & Nørskov, J. K. Electrochemical Barriers Made Simple. *J. Phys. Chem. Lett.*, 2663--2668 (2015).
38 Chan, K. & Nørskov, J. K. Potential Dependence of Electrochemical Barriers from ab Initio Calculations. *The Journal of Physical Chemistry Letters*, 1686-1690, doi:10.1021/acs.jpclett.6b00382 (2016).
39 Nørskov, J. K. *et al.* Origin of the Overpotential for Oxygen Reduction at a Fuel-Cell Cathode. *J. Phys. Chem. B* **108**, 17886--17892 (2004).
40 Wang, S. *et al.* Universal transition state scaling relations for (de)hydrogenation over transition metals. *Physical Chemistry Chemical Physics* **13**, 20760-20765, doi:10.1039/C1CP20547A (2011).
41 Yang, N. *et al.* Intrinsic Selectivity and Structure Sensitivity of Rhodium Catalysts for C2+ Oxygenate Production. *Journal of the American Chemical Society* **138**, 3705-3714, doi:10.1021/jacs.5b12087 (2016).
42 Medford, A. J. *et al.* Assessing the Reliability of Calculated Catalytic Ammonia Synthesis Rates. *Science* **345**, 197--200 (2014).
43 Kuhl, K. P., Cave, E. R., Abram, D. N. & Jaramillo, T. F. New insights into the electrochemical reduction of carbon dioxide on metallic copper surfaces. *Energy & Environmental Science* **5**, 7050-7059, doi:10.1039/C2EE21234J (2012).
44 Abild-Pedersen, F. *et al.* Scaling Properties of Adsorption Energies for Hydrogen-Containing Molecules on Transition-Metal Surfaces. *Physical Review Letters* **99**, 016105, doi:10.1103/PhysRevLett.99.016105 (2007).
45 Hatsukade, T., Kuhl, K. P., Cave, E. R., Abram, D. N. & Jaramillo, T. F. Insights into the electrocatalytic reduction of CO2 on metallic silver surfaces. *Physical Chemistry Chemical Physics* **16**, 13814-13819, doi:10.1039/C4CP00692E (2014).
46 Dahl, S. *et al.* Role of Steps in ${\mathrm{N}}_{2}$ Activation on Ru(0001). *Physical Review Letters* **83**, 1814-1817, doi:10.1103/PhysRevLett.83.1814 (1999).

47 Shi, C., Hansen, H. A., Lausche, A. C. & Nørskov, J. K. Trends in electrochemical CO2 reduction activity for open and close-packed metal surfaces. *Physical Chemistry Chemical Physics* **16**, 4720-4727, doi:10.1039/C3CP54822H (2014).
48 Schouten, K. J. P., Pérez Gallent, E. & Koper, M. T. M. The influence of pH on the reduction of CO and to hydrocarbons on copper electrodes. *Journal of Electroanalytical Chemistry* **716**, 53-57, doi:10.1016/j.jelechem.2013.08.033 (2014).
49 Roberts, F. S., Kuhl, K. P. & Nilsson, A. Electroreduction of Carbon Monoxide Over a Copper Nanocube Catalyst: Surface Structure and pH Dependence on Selectivity. *ChemCatChem* **8**, 1119-1124, doi:10.1002/cctc.201501189 (2016).
50 Kim, Y.-G., Javier, A., Baricuatro, J. H. & Soriaga, M. P. Regulating the Product Distribution of CO Reduction by the Atomic-Level Structural Modification of the Cu Electrode Surface. *Electrocatalysis*, 1-9, doi:10.1007/s12678-016-0314-1 (2016).
51 Matsushima, H., Taranovskyy, A., Haak, C., Gründer, Y. & Magnussen, O. M. Reconstruction of Cu(100) Electrode Surfaces during Hydrogen Evolution. *Journal of the American Chemical Society* **131**, 10362-10363, doi:10.1021/ja904033t (2009).
52 Zhu, W. *et al.* Active and Selective Conversion of CO2 to CO on Ultrathin Au Nanowires. *Journal of the American Chemical Society*, doi:10.1021/ja5095099 (2014).
53 Reske, R., Mistry, H., Behafarid, F., Roldan Cuenya, B. & Strasser, P. Particle Size Effects in the Catalytic Electroreduction of CO2 on Cu Nanoparticles. *Journal of the American Chemical Society* **136**, 6978-6986, doi:10.1021/ja500328k (2014).
54 Verdaguer-Casadevall, A. *et al.* Probing the active surface sites for CO reduction on oxide-derived copper electrocatalysts. *Journal of the American Chemical Society*, doi:10.1021/jacs.5b06227 (2015).
55 Peterson, A. A. & Nørskov, J. K. Activity Descriptors for CO2 Electroreduction to Methane on Transition-Metal Catalysts. *The Journal of Physical Chemistry Letters* **3**, 251-258, doi:10.1021/jz201461p (2012).